Ligational Properties of Two New Phenolic Aza Cages towards Proton and Alkali Metal Ions − a Theoretical and an Experimental Approach

Paolo Dapporto,[a] Mauro Formica,[b] Vieri Fusi,*[b] Luca Giorgi,[b] Mauro Micheloni,*[b] Roberto Pontellini,[b] Paola Paoli,*[a] and Patrizia Rossi[a]

Keywords: Synthesis / Aza cages / Crystal structures / Thermodynamics / Molecular dynamics

Molecular Dynamics (MD) simulations were performed on several species (anion, zwitterion, and neutral metal complexes) of two phenolic aza cages (**L1** and **L2**) in aqueous solution. The anionic species of the smaller **L1** ligand appears to be able to selectively encapsulate Li^+, while the other alkaline metal ions tested (Na^+ and K^+) are too large to be encapsulated. The larger cage **L2** does not show any selectivity; the anion binds all the alkaline metal ions. The two aza cages **L1** and **L2** were synthesized. Both basicity and alkali metal complex formation were studied in aqueous solution at 25 °C in 0.15 mol dm^{-3} Me_4NCl, using potentiometric, UV/Vis- and NMR-spectroscopic techniques. Both cages behave as triprotic bases in the pH range investigated; $\log K_1$ = 12.15(6), $\log K_2$ = 7.39(5), $\log K_3$ = 1.4(1) for **L1** and $\log K_1$ = 11.76(5), $\log K_2$ = 8.24(5), $\log K_3$ = 2.9(2) for **L2**. The last proton cannot be removed because both compounds are strongly basic under the experimental conditions studied. Proton localization was studied by UV/Vis and NMR spectroscopy, both in water and nonaqueous solutions. The crystal structures of [H**L1**](ClO_4) and [Na**L2**](ClO_4) were determined by X-ray analysis. The crystals of [H**L1**](ClO_4) are triclinic, space group $P(\bar{1})$; cell parameters are a = 10.3628(8), b = 11.938(1), c = 12.201(4) Å, α = 117.53(1), β = 101.25(1), γ = 102.774°. The crystals of [Na**L2**](ClO_4) are monoclinic, space group $P2_1/n$; cell parameters are a = 10.6154(7), b = 17.0418(9), c = 14.9452(9) Å, β = 95.634(6)°.

Introduction

The design of macrocyclic molecules to achieve selective host recognition is a widely used synthetic strategy.[1−6] To complex small, spherical guests such as metal ions, only macropolycyclic hosts are able to provide many binding sites directed towards the guest in a convergent manner, thus making the resulting metal complex thermodynamically stable. A further advantage of cage-like hosts is that solvation inside the cavity is weaker than with hosts where the binding sites are more exposed to the solvent.[7]

Alkali and alkaline earth cations are the simplest guests; they are spherical in shape and utilize only electrostatic forces for binding. In order to achieve selectivity among the alkali metal ions the size of the cavity of the macropolycyclic host should exactly match that of the alkali metal ion.

In our laboratory we have synthesized many small aza cages,[8−22] some of which are able to selectively encapsulate the lithium ion.[11,13,15,17,18] In some cases these molecules behave as "*fast proton sponges*",[8,9,11,12,19] indicating that the smallest cation, the proton, is also selectively encapsulated. In order to gain spectroscopic information about the binding event, chromoionophores such as nitro and/or phenolic groups have been inserted into the molecular frameworks.[23−26] One of the latest small aza cages studied in our laboratories thus far is compound **L** (see Scheme 1).[27] The ligand is able to selectively encapsulate the lithium ion, a $\log K > 3$ is expected for the complexation process $Li^+ + [H_{-1}L]^- = [LiH_{-1}L]$.[27] At 300 K the molecule, both in the $[H_2L]^{2+}$ [27] and the $[H_{-1}L]^-$ species, appeared rather rigid in the MD simulations performed in aqueous solution [the solvent was mimicked by using a distance-dependent dielectric constant $\varepsilon(r) = 80r$, unpublished results]. In particular, the phenolic moiety does not change its orientation with respect to the [12]aneN_4 ring. It is almost parallel to the *trans*-dimethylated tetraazamacrocycle with the oxygen atom pointing "outside" the macrobicyclic cavity. We designed the trial molecules **L1** and **L2** (see Scheme 1) starting from this molecule, with the aim to obtain a more flexible macrobicyclic skeleton which can better accommodate the donors around the metal guest. The promising theoretical results obtained encouraged us to synthesize these two new molecules. Their ligational properties towards proton (i.e. their basicity) and alkali metal ions were investigated both in solution (by potentiometric titrations, UV/Vis and NMR spectra) and in the solid state (by

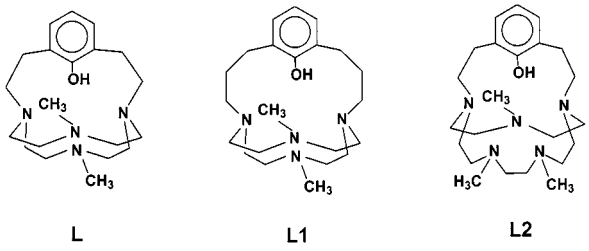

Scheme 1. Drawing of the ligands

[a] "Sergio Stecco" Department of Energy Engineering, University of Florence,
Via S. Marta No. 3, 50139 Florence, Italy
[b] Institute of Chemical Sciences, University of Urbino,
Piazza Rinascimento No. 6, 61029 Urbino, Italy
Fax: (internat.) + 39-0722/350032
E-mail: mauro@chim.uniurb.it

  1434−1948/01/0707−1763 $ 17.50+.50/0

X-ray diffraction), and then compared with the modeled behavior.

Results and Discussion

Molecular Dynamics Simulations

(i) *Anion Species*

During the MD simulation of $[H_{-1}\mathbf{L1}]^-$, the dominant conformation was found to be characterized by a phenolate group which is nearly parallel to the mean plane described by the four nitrogen atoms. In this case, the oxygen atom of the bridging unit is always directed towards the methyl moiety disposed above the *trans*-dimethylated cyclen ring. As a consequence, during the MD run at least one $-CH_3\cdots O$ intramolecular interaction (< 2.7 Å) takes place. The two *trans*-disposed methyl groups point in opposite directions with respect to the [12]aneN$_4$ mean plane, with the exception of just a few conformations. Figure 1 (a) reports the average structure from snapshots of the coordinates for $[H_{-1}\mathbf{L1}]^-$. However, during the simulation time a few conformations were observed to have the phenolate moiety almost perpendicular to the [12]aneN$_4$ ring. As expected, the propyl chains allow the phenolate ring greater conformational freedom relative to the ligand **L**. In this regard the $[H_{-1}\mathbf{L2}]^-$ anion is more rigid, with the benzene ring always in the same orientation with respect to the 15-membered ring. Thus, the lengthening of the polyaza ring does not provide greater conformational freedom of the bridging moiety. As in **L** and **L1**, the phenolate ring of **L2** is almost parallel to the N_5 mean plane and the oxygen atom is oriented towards the longer chain bearing the two methyl groups of the [15]aneN$_5$ base. The latter groups are always pointing in the opposite direction to the [15]aneN$_5$ ring, while the third methyl group is always positioned below the mean plane. Figure 1 shows the average conformation resulting from MD. Furthermore, the collected conformations show at least one intramolecular interaction between the phenolic oxygen atom and a hydrogen atom of a methyl group.

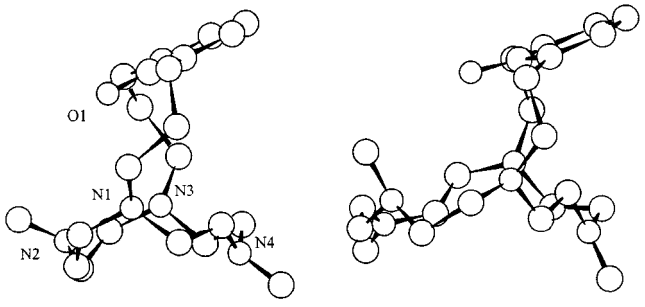

Figure 1. Average conformation from snapshots of coordinates for (a) $[H_{-1}\mathbf{L1}]^-$, (b) $[H_{-1}\mathbf{L2}]^-$

In order to evaluate the approximate size of the three-dimensional cavity inside the two macrocyclic ligands that is able to accommodate the cation, the distances between the geometric center defined by the donors and each donor atom itself were calculated throughout the simulations. Table 1 lists these average distances for the $[H_{-1}\mathbf{L1}]^-$ and $[H_{-1}\mathbf{L2}]^-$ species, as well as an estimate of the metal–donor bond lengths obtained from crystal structures of metal ($M = Li^+$, Na^+, and K^+) complexes having nitrogen and/or oxygen atoms as donors, which have been deposited at the CCDC.[28] With regard to the $[H_{-1}\mathbf{L1}]^-$ ligand, comparison between the distance values reported in Table 1 seems to indicate that the molecular cavity is too small to encapsulate the sodium and potassium ions, whereas it is well suited to the size of the Li^+ ion. On the contrary, the donors of the larger $[H_{-1}\mathbf{L2}]^-$ host appear to be suitable to bind the sodium and potassium cations, while the lighter lithium is probably too small.

Table 1. Mean X (center of donors)–donor atoms distances [Å] obtained from MD simulations and mean metal–donor bond lengths [Å] obtained from the crystal structures of the metal ($M = Li^+$, Na^+, and K^+) complexes having nitrogen and/or oxygen atoms as donors deposited at the CCDC

$[H_{-1}\mathbf{L1}]^-$	$[H_{-1}\mathbf{L2}]^-$	Li^+ donor	Na^+ donor	K^+ donor
X–O1 2.78	X–O1 2.61	Li–N 2.2	Na–N 2.5	K–N 2.8
X–N1 2.21	X–N1 2.63	Li–O 2.1	Na–O 2.4	K–O 2.8
X–N2 2.16	X–N2 2.80			
X–N3 2.15	X–N3 2.95			
X–N4 2.71	X–N4 2.72			
	X–N5 3.05			

(ii) *Neutral Species*

Both cages in their neutral form still contain one proton and are zwitterions. The acidic hydrogen atom (H1) was bound to a bridgehead nitrogen atom, as found in previous work involving similar monoprotonated cages.[29] Once again, during the MD runs the phenolate ring is almost coplanar to the N_4 and N_5 mean planes of **L1** and **L2**, respectively. However, in **L1** the propyl chains connecting the phenolate group to the [12]aneN$_4$ are more stretched out than in the anionic form. As a result, the phenolic oxygen atom is further from the mean N_4 plane in **L1** than in $[H_{-1}\mathbf{L1}]^-$ (see Figure 2, a), and the stabilization of the zwitterion can be entirely ascribed to the nitrogen atoms (vide infra). Conversely, the introduction of an acidic proton within the molecular framework of $[H_{-1}\mathbf{L2}]^-$ does not significantly affect the overall shape of the molecule, the only noteworthy difference is that the two adjacent methylated nitrogen atoms are always pointing above the N_5 mean plane (see Figure 2, b).

In order to gain some information concerning the relative basicity of both compounds in the reaction $[H_{-1}L]^- + H^+ \rightarrow L$, the inter-atomic distances of the H···donor atoms were collected during the simulations. In both zwitterions, the acidic proton appears to be involved in essentially two H-bonding interactions (see Table 2). In **L1** the acidic hydrogen atom interacts more closely with the two methylated nitrogen atoms. The interaction with the phenolic oxygen atom is weaker as it is more distant. Most conformations of the larger compound **L2**, show an N–H···O hydrogen

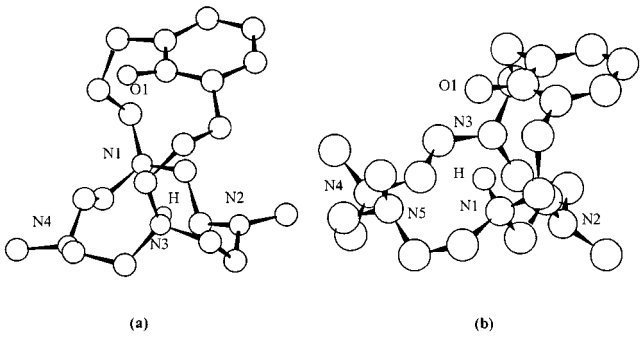

Figure 2. Average conformation from snapshots of coordinates for (a) [**L1**], (b) [**L2**]

Table 2. Mean H−donor atoms distances [Å] obtained from MD simulations

L1	**L2**
H−O1 4.15	H−O1 2.34
H−N1 3.61	H−N2 3.92
H−N2 2.41	H−N3 3.92
H−N4 2.62	H−N4 4.46
	H−N5 2.66

bond and an interaction involving the closer methylated nitrogen atom N5 belonging to the longer arm of the [15]aneN$_5$ ring. In both forms the mean H···acceptor distances are very similar; as a result, we can infer that the basicity properties of the two polyaminic bases should be similar.

(iii)−(iv) *Metal Complexes*

The results from the simulations performed in the two media studied are practically identical. Table 3 reports the average distances of the M−donors extracted from the MD simulations. In both cases [H$_{-1}$**L1**]$^-$ appears to be able to bind only the smallest alkaline cation. The sodium ion comes out from the molecular cavity, remaining close to the phenolic oxygen atom throughout the entire simulation time (mean Na−O distance 2.22 Å). The largest ion, potassium, moves away from the macrocycle very quickly, thus confirming the results of the preliminary studies concerning the cavity size of the ligands in the anionic form. The mean Li−N distances monitored during the MD run ranged from 2.09 to 2.34 Å. The phenolic oxygen atom interacts strongly with the lithium cation. The mean Li−O distance is 1.75 Å, with the Li−O bond pointing inside the molecular cavity. As a result of this interaction, the phenyl ring is almost perpendicular to the N$_4$ ring and the overall shape of the metal complex is different from that observed for the anion and the zwitterion (see Figure 3, a). The coordination geometry around the metal guest is trigonal-bipyramidal, with the bridgehead nitrogen atoms occupying the axial positions, as already found in the solid-state X-ray structures of analogous tbp macrobicycle−Li$^+$ complexes (SEKSAC[15a] and SONJAC[17] refcode). In the latter complexes, all the donor atoms were nitrogen atoms and the Li−N distances were shorter (mean 2.04 Å) than in [LiH$_{-1}$**L1**]. Furthermore, in the lithium complex with 4,7,13-trioxa-1,10-diazabicyclo[8.5.5]icosane (FENHIP[30]), whose chain lengths are comparable with those of **L2**, the coordination distances are very similar to those observed during the MD simulation of [LiH$_{-1}$**L2**] (vide infra).

Table 3. Mean M−donor atoms distances [Å] obtained from MD simulations

H$_{-1}$**L1**	LiH$_{-1}$**L2**
Li−O1 1.75	Li−O1 1.81
Li−N1 2.34	Li−N1 2.79
Li−N2 2.09	Li−N2 2.29
Li−N3 2.21	Li−N3 2.44
Li−N4 2.13	Li−N4 2.17
	Li−N5 2.90
NaH$_{-1}$L2	**KH$_{-1}$L2**
Na−O1 2.15	K−O1 2.51
Na−N1 2.66	K−N1 2.76
Na−N2 2.47	K−N2 2.72
Na−N3 2.59	K−N3 2.72
Na−N4 2.63	K−N4 2.71
Na−N5 2.44	K−N5 2.63

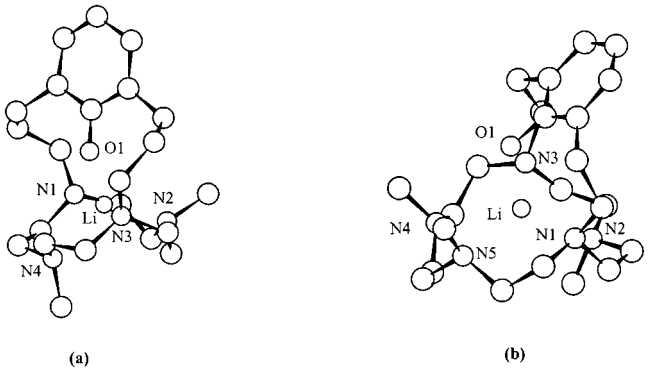

Figure 3. Average conformation from snapshots of coordinates for (a) [Li**L1**], (b) [Li**L2**]

The [H$_{-1}$**L2**] species behaved in a similar manner towards the lithium, sodium, and potassium cations. During the MD runs the cation was encapsulated within the ligand cavity in all cases. These results seem to indicate that the larger ligand is not a selective binder of the lithium ion. In the [LiH$_{-1}$**L2**] complex the mean Li−N distances range from 2.2 to 2.9 Å, with a mean Li−O bond length of 1.8 Å (see Table 3). Essentially, the molecular cavity appears to be too large to accommodate the smallest alkaline cation, while the monitored M−donor distances for the sodium and potassium complexes are in agreement with the corresponding experimental values retrieved from the CCDC. In terms of bond lengths, the coordination of the lithium ion appears to be of the 4+2 type which is in agreement with the trend observed in the solid-state structures of hexacoordinated Li$^+$−macrobicyclic complexes with nitrogen and/or oxygen donor atoms, retrieved from the CCDC.

The phenyl ring gradually changes its orientation with respect to the N_5 mean plane, in the lithium complex it is almost perpendicular, while in the potassium one it is almost coplanar (see Figure 3, b, and Figure 4).

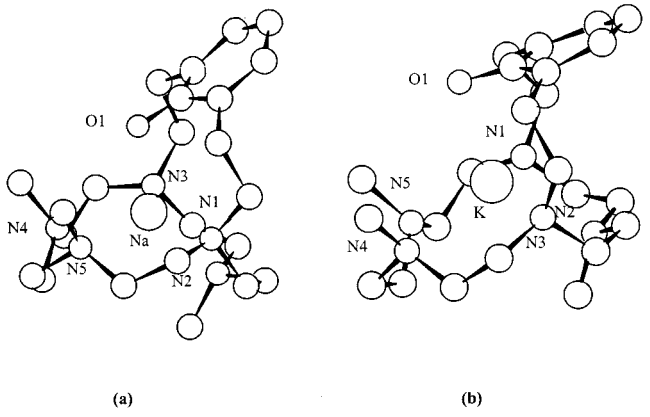

Figure 4. Average conformation from snapshots of coordinates for (a) [Na**L2**], (b) [K**L2**]

Synthesis

The cages **L1** and **L2** were prepared according to the synthetic procedures depicted in Figure 5. The two cages were obtained by following the synthetic procedure reported for the analogous phenolic aza cage **L**.[25] This procedure involves the use of a dimesyl derivative of 2,6-dimethylanisole, and of an aza crown base as the reactants to increase the 1 + 1 product in the final cyclization. In order to obtain **L2**, the new aza crown base **7** was synthesized (see Figure 6). The synthesis of **7**, according to the Richman–Atkins method, requires the use of the ditosylated polyamine **3**, obtained by the extension of *N*,*N*′-dimethylethylendiamine (**1**) with 2 equiv. of *N*-(*p*-tolylsulfonyl)aziridine (**2**). The reaction of the disodium salt of **3** with bis(2-chloroethyl)methylamine (**5**) in DMF leads to the ditosylated macrocycle **6**, which was detosylated with strong acid giving **7**. By treating the aza base **7** with methyl 2-[2-methoxy-3-(2-methylsulfonyloxyethyl)phenyl]ethanesulfonate (**16**) in acetonitrile in the presence of an alkaline carbonate base, we obtained the phenol-protected cage **18** (see Figure 5). To synthesize the cage **L1**, a longer dimesyl derivative **15** of 2,6-dimethylanisole was prepared (see Figure 7). In order to obtain reagent **10**, which is the starting material used to prepare **15**, we followed a different synthetic scheme than that reported previously,[31] thus achieving a higher reaction yield. Compound **15** was obtained from **10** using a classic elongation method of an alkyl chain. The cyclization of **15** with the macrocyclic aza base **17**, gives the phenol-protected cage **19**. For both ligands **18** and **19**, no template effect was found in the cyclization step; moreover, they were deprotected in the same way, with sodium ethanethiolate in DMF. This afforded the phenolic aza cages **L1** and **L2**, after the purification steps.

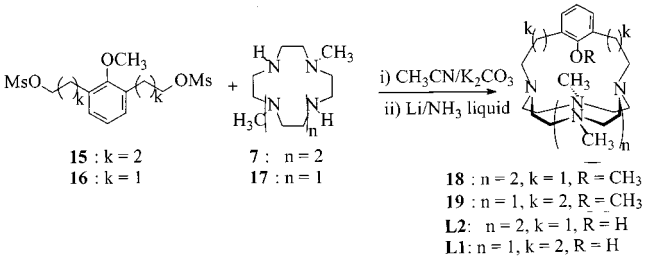

Figure 5. Synthetic pathway used to obtain compounds **L1** and **L2**

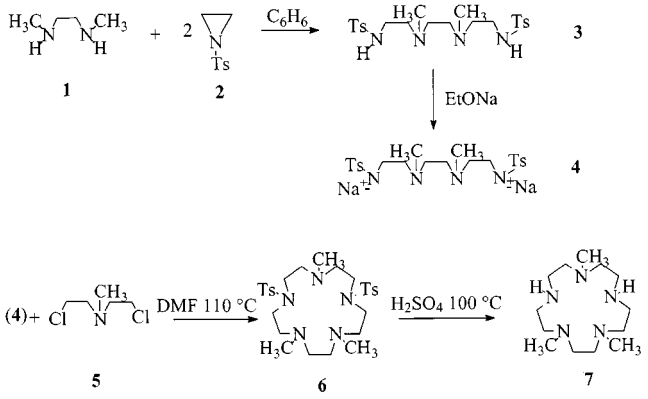

Figure 6. Synthetic procedure to obtain macrocycle **7**

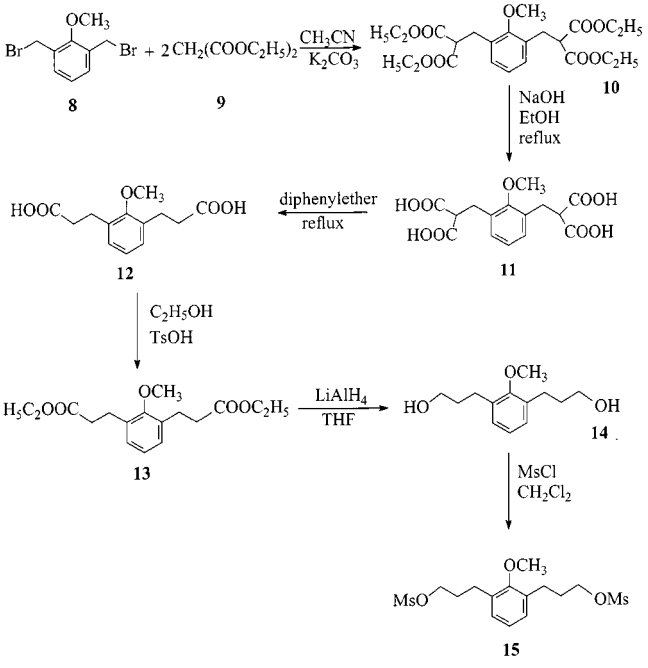

Figure 7. Synthetic procedure to obtain intermediate compounds for the synthesis of **L1**

Protonation and Complex Formation Equilibria

Table 4 reports the protonation constants of **L1** and **L2**. The ligands have a total of five and six protonation sites respectively, and all of the nitrogen atoms are tertiary. Both cages accept three protons under the experimental conditions employed. It should be noted that both cages in their neutral species still contain one proton. This proton cannot be removed in the pH range investigated because the fully deprotonated species $[H_{-1}\mathbf{L1}]^-$ and $[H_{-1}\mathbf{L2}]^-$ are strongly

basic. As expected, the molecular topology strongly influences the basicity behavior of **L1** and **L2**; both compounds are much stronger bases than both the phenolate and the polyaminic tertiary nitrogen atom.[32]

Table 4. Protonation constants of **L1** and **L2** (log *K*) determined by potentiometry in 0.15 mol dm^{-3} Me_4NCl aqueous solution at 298±0.1 K

Reaction	**L1**	**L2**
$L + H^+ = HL^+$	12.15(6)[a]	11.76(5)
$HL^+ + H^+ = H_2L^{2+}$	7.39(5)	8.24(5)
$H_2L^{2+} + H^+ = H_3L^{3+}$	1.4(1)	2.9(2)

[a] Values in parentheses are the standard deviation to the last significant figure.

In order to understand how the phenolic moiety is involved in the protonation steps, absorption electronic spectra and NMR experiments were performed on the compounds **L1** and **L2** in water and in nonaqueous solvents. For both ligands, the absorption and NMR spectra show the involvement of the phenolic group in the protonation steps. For example, the UV spectra of **L1** recorded in aqueous solution, are different in acidic and basic solution. The spectrum shows a band with λ_{max} = 272 nm ($\varepsilon_{\lambda max}$ = 950 M^{-1} cm^{-1}) in the acidic region, while at a pH value slightly over 12, where the neutral species is prevalent in solution, two bands appear in the spectra at λ_{max} = 239 ($\varepsilon_{\lambda max}$ = 5900 M^{-1} cm^{-1}) and 295 nm ($\varepsilon_{\lambda max}$ = 2600 M^{-1} cm^{-1}). This latter spectrum is also maintained at more alkaline pH values. The different behavior of the chromophore in the acidic and basic solution is due to the presence of the phenol hydroxy form at low pH values and to the phenolate form at high pH values. This spectral feature suggests that in the neutral species the ligand is in the zwitterionic form in aqueous solution, with the acidic proton located on the aza base. ^1H NMR spectra of **L1** recorded in aqueous solution, confirmed this hypothesis. The spectrum at pH = 2 in fact shows broad resonances in the aliphatic field, while the aromatic protons give rise to a doublet at δ = 7.15 integrating for two protons (the aromatic protons in *meta* position), and a triplet at δ = 7.00 integrating for one proton (the aromatic proton in *para* position). These resonances undergo an upfield shift in the spectrum recorded at pH = 12, resonating at δ = 6.86 and 6.38 for the doublet and the triplet, respectively. This indicates the deprotonation of the phenolic group at alkaline pH values. Compound **L2** shows a similar behavior with very small differences in wavelengths and in chemical shifts.

The behavior of **L1** and **L2** is different in methanol. The absorption spectra for the phenolic group do not change significantly in acidic or strong alkaline solution, the maximum wavelength and molar absorptivity remain the same [one band with λ_{max} = 276 nm (ε = 1400 M^{-1} cm^{-1})]. In other words, the phenolic group appears in its hydroxy form even in the neutral species. This behavior was also found for **L**, as already reported,[27] and can be explained by the different solvating power of the two media; the charge−charge separation in water is successful, however, in methanol it is not. Nevertheless, it was possible to record the spectrum of the $[H\mathbf{L1}]^+$ species in methanol which shows a different absorption spectrum from the previous ones. Two bands appear at λ_{max} = 236 nm ($\varepsilon_{\lambda max}$ = 4300 M^{-1} cm^{-1}) and λ_{max} = 292 nm ($\varepsilon_{\lambda max}$ = 700 M^{-1} cm^{-1}). The spectrum is similar to that recorded in aqueous solution at an alkaline pH value, highlighting the presence of the phenolate form in the $[H\mathbf{L1}]^+$ species in methanol.

^1H and ^{13}C NMR spectra were recorded to better analyze the $[H\mathbf{L1}]^+$ species in solution. The ^1H NMR spectrum of the $[H\mathbf{L1}]^+$ species, carried out in $CDCl_3$, is shown in Figure 8a. It shows a broad deshielded resonance at δ = 9.97 integrating for two protons which can be assigned to the acidic protons of the ligand. After the addition of a small amount of H_2O or CH_3OH to the chloroform solution, the signal remains. This indicates a slow exchange, on the NMR time scale, of the two protons with the mobile protons of the solvent. However, when D_2O or CD_3OD was added the resonance disappeared. These experimental data suggest that the two protons are positioned inside the macrocyclic cavity and are stabilized by a strong hydrogen-bonding network involving the donor functions. This is in agreement with the X-ray structure (vide infra). The ^1H NMR spectrum of the same species recorded in CD_3OD (Figure 8, b) reveals the disappearance of the deshielded resonance, while the pattern of the other resonances remain quite similar. The addition of Me_4NOH to the species $[H\mathbf{L1}]^+$ in CD_3OD solution (Figure 8, c) leads to a downfield shift of the triplet

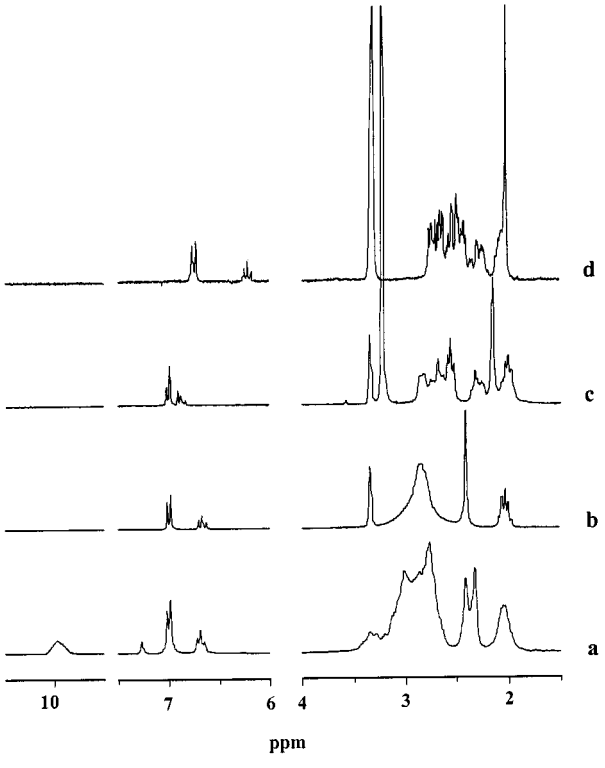

Figure 8. (a) The ^1H NMR spectrum of $[H\mathbf{L1}]^+$ in $CDCl_3$, (b) ^1H NMR spectrum of $[H\mathbf{L1}]^+$ in CD_3OD, (c) ^1H NMR spectrum after the addition of Me_4NOH, (d) ^1H NMR spectrum of $[LiH_{-1}\mathbf{L1}]$ in CD_3OD

due to the aromatic proton in the *para* position, together with an upfield shift of almost all the aliphatic resonances, thus indicating the loss of positive charge density on the amine groups and the protonation of the phenolate oxygen atom. This is in agreement with the UV spectra. In conclusion we can say that in the $[H\mathbf{L1}]^+$ species, the nature of the acidic proton, in water and in organic solvents, seems to be the same as that found in the solid state. In organic solvents the removal of one proton results in the redistribution of the last acidic proton, it is located on the oxygen atom. However, in aqueous solution the last acidic proton remains on the aza base. The ^{13}C NMR spectra recorded in the same solvents, also support this hypothesis. Moreover, **L2** and the smallest compound **L** display similar behavior.[27]

Alkali Metal Ions Complexation

The coordination of the alkali metal ions by ligands **L1** and **L2** was also investigated by ^1H, ^{13}C, and ^7Li NMR spectroscopy and by UV/Vis absorption electronic spectra in water and in organic solvents. Potentiometry was also employed to investigate the formation equilibria of alkali metal complexes (see Table 5). The equilibrium constants reported in Table 5 refer to an overall process in which the alkali metal ion M^+ is bound and, at the same time, the last proton present in the cages is removed, yielding a neutral species $MH_{-1}L$ [$M^+ + L = MH_{-1}L + H^+$]. The stability constants relative to the net complexation process $M^+ + H_{-1}L^- = MH_{-1}L$ can only be estimated since the first protonation constant for both cages **L1** and **L2** is too high to be measured under the chosen experimental conditions. The log*K* value for the first protonation step $H^+ + H_{-1}L = L$ should be greater than 12.15 and 11.76 for **L1** and **L2**, respectively. Also, log*K* > 4 and log*K* > 3 are expected for the net complexation process ($Li^+ + H_{-1}L^- =$ LiL) for **L1** and **L2**, respectively, since the values for the complexation of Li^+ (8.03 and 8.91, see Table 5) should be subtracted. For cage **L2** all three metal ions can be complexed, potentiometric studies show that the estimated stability constants are very similar (see Table 5). For ligand **L1**, the spectroscopic experiments do not reveal any complex formation with sodium and potassium ions in water or in the alcohol solution. **L1** does form a complex with the smallest ion Li^+ and the complex was also isolated in the solid state. As is often the case with aza cage lithium complexes,[11,13,15,17,18] the solid complex is soluble in organic solvents such as $CDCl_3$. The ^7Li NMR spectrum shows a sharp peak which is shifted downfield (0.53 ppm) with respect to that of the free Li^+ ion. The spectra of $[LiH_{-1}\mathbf{L1}]$ show the same signal with an approximately equal chemical shift both in water and in methanol. When an excess amount of Li^+ is added to the solution of the complex, the ^7Li NMR spectrum shows the appearance of a new sharp peak at $\delta = 0$ due to the free lithium ion, together with that of the complexed lithium ion. The simultaneous presence of two peaks in the spectrum denotes a slow exchange (on the NMR time scale) of the complexed lithium ion with the free lithium. The independence of the ^7Li chemical shift from the solvent, and the slow exchange on the NMR time scale between the free and bound lithium ion suggest that it is encapsulated inside the macrocyclic cavity and hence is quite isolated from the medium. The ^1H NMR spectrum of the $[LiH_{-1}\mathbf{L1}]$ in CD_3OD (see Figure 8 spectrum d) shows a marked upfield shift of the triplet signal due to the aromatic proton in the *para* position relative to that of the neutral species (see Figure 8 spectrum c). This suggests the deprotonation of the phenol group with lithium complexation. The ^1H NMR spectrum of the lithium complex recorded in aqueous solution shows broader signals with approximately the same chemical shifts in the resonances. The UV spectra recorded in water and in methanol of the lithium complex show the two characteristic bands of the phenolate form with an increased molar absorptivity in water with respect to the free ligand at the same pH values [λ_{max} = 241 nm ($\varepsilon_{\lambda max}$ = 8250 M^{-1} cm^{-1}), λ_{max} = 296 nm ($\varepsilon_{\lambda max}$ = 4200 M^{-1} cm^{-1})].

Table 5. Logarithms of the equilibrium constants determined in 0.15 mol dm^{-3} Me_4NCl at 298.1 K for the complexation reactions of **L1** and **L2** with Li^+, Na^+, and K^+ ions

	Li^+	Na^+	K^+
$M^+ + \mathbf{L1} = MH_{-1}\mathbf{L1} + H^+$	−8.03	–	–
$M^+ + \mathbf{L2} = MH_{-1}\mathbf{L2} + H^+$	−8.91	−8.33	−8.65

A different behavior is shown by the larger compound **L2**. No selectivity was found in aqueous solution by the spectroscopic techniques which is in agreement with the MD simulations. However, some interesting aspects were revealed. The ^7Li NMR spectra recorded in aqueous solution and in methanol show only one signal that rapidly interchanges with the free lithium ion, thus denoting the easy access of the solvent to the ion sphere, together with the poor fit of the ion in the macrocyclic cavity as previously inferred from MD simulation results. In both media, the ^1H NMR spectra of the $[MH_{-1}\mathbf{L2}]$ metal complexes reveal the lack of selectivity of the ligand; for example, the spectrum of each complex can also be obtained by adding a small excess of the metal ion to a solution of another complex. However, some interesting results were found in the case of the sodium complexes. Solution studies performed in methanol in fact reveal that the $[Na\mathbf{L2}]^+$ species, which is probably in a conformation similar to that found in the crystal structure, rapidly evolves into another species upon addition of a small amount of a base. This is well depicted by monitoring the aromatic region of the ^1H NMR spectra of $[Na\mathbf{L2}]^+$ and the UV/Vis absorption electronic spectra of these species (Figure 9). The new species corresponds to that of the $[NaH_{-1}\mathbf{L2}]$ sodium complex which is isolated in the solid state as reported in the Exp. Sect. As depicted in the aromatic part of the ^1H NMR spectrum of the $[NaH_{-1}\mathbf{L2}]$ species, there are two stable conformers on the NMR time scale that give rise to a high number of signals in the ^{13}C NMR spectra as well (see Exp. Sect.). However, in both conformers, the upfield shift of the proton located

in the *para* position, as compared with that in the $[NaL2]^+$ spectrum, suggests the deprotonation of the phenolic group of **L2** due to metal complexation. This hypothesis was confirmed by the comparison of the UV spectra of the $[NaL2]^+$ and $[NaH_{-1}L2]$ complexes, each of which has the spectral characteristics of one of the two forms of the phenol, thus suggesting a conformation of $[NaL2]^+$ in solution which is similar to that found in the solid state and leading to the deprotonation of the ligand in more basic solutions.

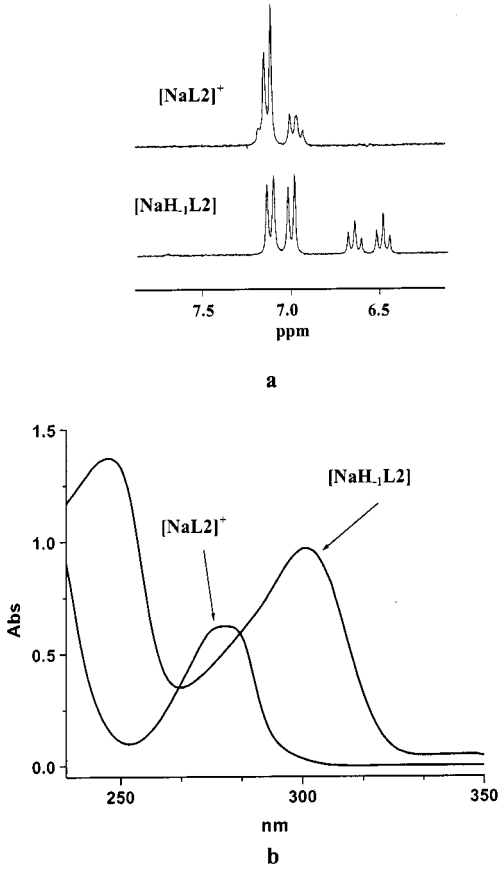

Figure 9. (a) The ^1H NMR spectra of the Na^+/**L2** system, (b) UV/Vis absorption electronic spectra of $[NaL2]^+$ and $[NaH_{-1}L2]$

X-ray Structures

$[HL1]^+(ClO_4)^-$

The crystal structure consists of $[HL1]^+$ cations and $(ClO_4)^-$ anions. Figure 10 shows an ORTEP[33] view of the $[HL1]^+$ cation with the atom labelling. Crystal and structure refinement data are reported in Table 6. With regard to the protonation sites, the two acidic hydrogen atoms are bound to the bridgehead nitrogen atoms N1 and N3 and form short hydrogen bonds with the oxygen atom O1 [H1N···O1 1.70(7), H3N···O1 1.79(6) Å]. The interactions between these hydrogen atoms and the other two donor atoms (N2 and N4) are significantly weaker than those involving the oxygen atom with distances 2.56(7) and 2.90(7) Å for [H3N···N2] and [H1N···N2], respectively, and 2.67(5) and 2.79(5) Å for [H1N···N4] and [H3N···N4], respectively. The atoms N1 and N3 are pointing toward the phenolic group. The nitrogen atoms N2 and N4 are on the opposite side of the N_4 mean plane, with their bonded methyl groups equatorial and axial with respect to the N_4 mean plane, respectively. In the crystal there are no strong intermolecular interactions. The conformation assumed by the [12]aneN$_4$ ring is of the [2424] C-corners type.[34] This is not a very common conformation for this class of compounds; in fact, the analysis of the solid-state structures collected in the Cambridge Structural Database v.5.19 revealed that the most common conformation assumed by [12]aneN$_4$ diprotonated rings is [3333].

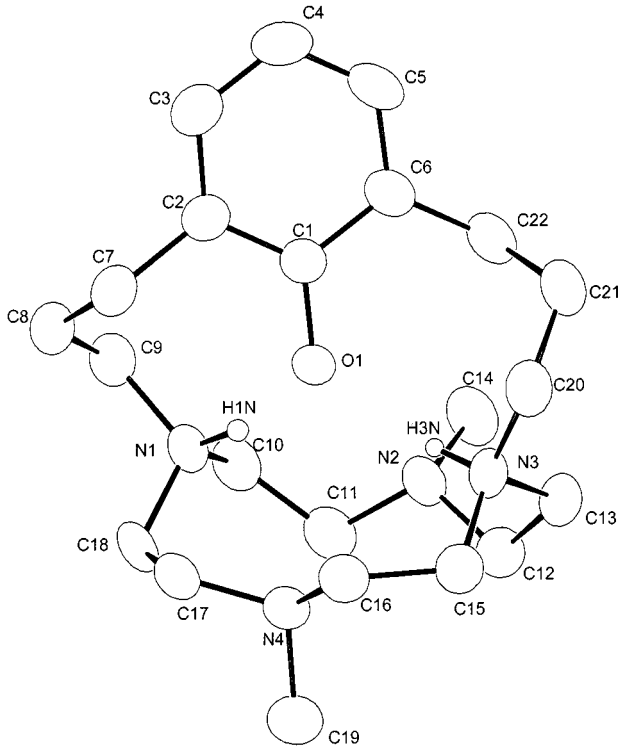

Figure 10. ORTEP view of the $[HL1]^+$ cation

Table 6. Crystal data and structure refinement for $[HL1](ClO_4)$ and $[NaL2](ClO_4)$

Empirical formula	$C_{22}H_{39}ClN_4O_5$	$C_{23}H_{41}ClN_5NaO_5$
Molecular mass	475.02	526.05
Temperature [K]	293	293
λ [Å]	1.5418	1.5418
Crystal system, space group	triclinic, $P(\bar{1})$	monoclinic, $P2_1/n$
Unit cell dimensions[Å, °]	a = 10.3628(8), α = 117.53(1) b = 11.938(1), β = 101.25(1) c = 12.201(4), γ = 102.774(9)	a = 10.6154(7) b = 17.0418(9), β = 95.634(6) c = 14.9452(9)
Volume [Å^3]	1225.9(9)	2690.6(2)
Z	2	4
Calculated density [g/cm^3]	1.287	1.299
μ [mm^{-1}]	1.706	1.763
Final R indices [$I > 2\sigma(I)$]	$R1$ = 0.0519, $wR2$ = 0.1408	$R1$ = 0.0682, $wR2$ = 0.1948
R indices (all data)	$R1$ = 0.0653, $wR2$ = 0.1564	$R1$ = 0.0848, $wR2$ = 0.2135

$[NaL2]^+(ClO_4)^-$

The structure consists of $[NaL2]^+$ cations and of $(ClO_4)^-$ anions. Figure 11 shows a perspective view of the complex cation. In Table 6 crystal and structure refinement data are reported. Selected bond lengths and angles are given in Table 7. The sodium ion is bound to the five nitrogen atoms of the ligand and to the oxygen atom of the phenol group. The coordination geometry around the sodium ion can be described as a strongly distorted pyramid having a pentagonal base, with the apex occupied by the oxygen atom. The five nitrogen atoms at the corners of the pentagonal base are not in a plane as seen by the deviations from the mean plane passing through them [minimum deviation 0.045(3) Å (N5), maximum deviation 0.750(3) Å (N3), mean deviation 0.507(3) Å]. The Na−N distances range from 2.455(3) to 2.731(3) Å. It is worthy to note that the two bridgehead nitrogen atoms are significantly further (see Table 7), perhaps because of the conformational requirements of the ethylenic chains connecting the phenol ring to the 15-membered macrocycle. The complex cation possesses a pseudo-symmetry plane crossing the phenol moiety and the bond between the C17 and C18 atoms. In this plane lie the Na, N2, and O1 atoms. An examination of the dihedral angles of the macrobicycle shows that the greatest deviation from this pseudo-symmetry is due to the N4−C17−C18−N5 fragment; the dihedral angle around N4−C17 is −175°, versus a value of 96° for the angle about the N5−C18 bond. The phenol ring forms an angle of 18.4(1)° with the N_5 mean plane. Both the methyl groups bound to N4 and N5 are pointing towards the same side of the N_5 ring, with the other methyl group (bound to N2) pointing in the opposite direction. This is in agreement with the results of MD simulations performed on the zwitterionic species. No interesting intramolecular interactions were observed, while a short intermolecular interaction between the hydrogen atom of the phenol group and an oxygen atom of the perchlorate anion was observed [O1−H10····O2 = 2.09(4) Å].

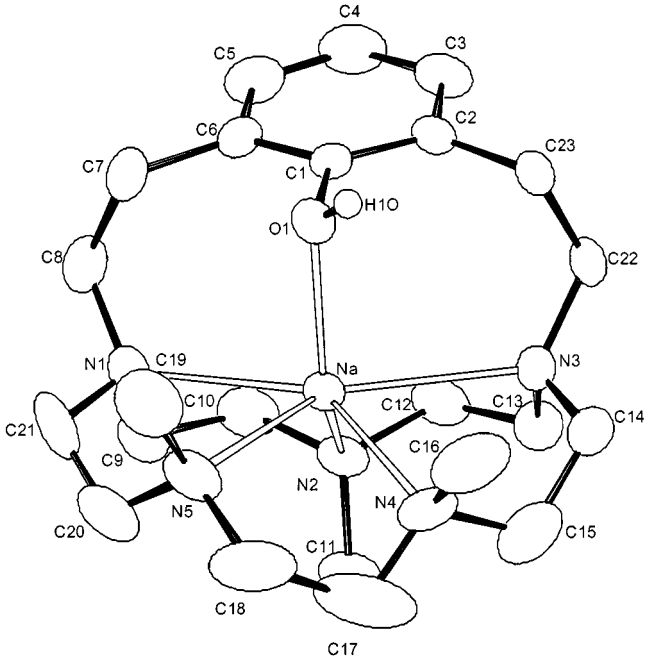

Figure 11. ORTEP view of the $[NaL2]^+$ complex

Table 7. Selected bonds lengths [Å] and angles [°] for $[NaL2]^+$

Na−O(1)	2.301(3)
Na−N(4)	2.455(3)
Na−N(2)	2.473(3)
Na−N(5)	2.504(3)
Na−N(1)	2.667(3)
Na−N(3)	2.731(3)
O(1)−Na−N(4)	109.61(11)
O(1)−Na−N(2)	132.82(10)
N(4)−Na−N(2)	108.91(12)
O(1)−Na−N(5)	94.87(12)
N(4)−Na−N(5)	73.05(16)
N(2)−Na−N(5)	121.84(13)
O(1)−Na−N(1)	91.30(11)
N(4)−Na−N(1)	141.78(14)
N(2)−Na−N(1)	74.24(12)
N(5)−Na−N(1)	73.62(15)
O(1)−Na−N(3)	93.60(10)
N(4)−Na−N(3)	72.59(13)
N(2)−Na−N(3)	73.15(11)
N(5)−Na−N(3)	145.49(15)
N(1)−Na−N(3)	139.54(13)

Experimental Section

General Remarks: ^1H, ^{13}C, and ^7Li NMR spectra were recorded with a Bruker AC-200 instrument, operating at 200.13, 50.33, and 77.78 MHz, respectively. In the ^1H NMR experiments peak positions are reported in relation to HOD ($\delta = 4.75$) and dioxane was used as the reference in the ^{13}C NMR spectra ($\delta = 67.4$). ^7Li peaks are reported in relation to free $LiClO_4$. ^1H-^1H and ^1H-^{13}C correlation experiments were performed to assign the signals. Solvents and starting products were used as purchased.

Molecular Dynamics (MD) Simulation Protocol: The studied species were the anions $[H_{-1}L1]^-$ and $[H_{-1}L2]^-$, the neutral ligands **L1** and **L2** (zwitterionic forms) and the neutral metal complexes $M[H_{-1}L1]$ and $M[H_{-1}L2]$ ($M = Li^+$, Na^+, and K^+). The MSI software programs InsightII and Discover version 98.0[35] were used for all the molecular modeling studies. Based on the good results of a previous computational study performed on monoprotonated macrocyclic compounds[29] of the same family, the Amber[36] force field was used (all the 1−4 nonbonding interactions were scaled by a factor of 0.5). Atomic charge distributions were calculated according to the ChelpG scheme at the single point 6−31G* level of theory using Guassian94 (revision D3).[37] As initial geometries for each species in vacuo, fully optimized model-built structures were used. In addition, before starting with the MD procedures the initial molecular assembly was further optimized until the convergence criterion was met (< 0.01 kcal mol^{-1}). The MD simulation temperature was set at 298 K and the Verlet leapfrog algorithm, with a time step of 1 fs, was used for integration of equations of motion in all simulations. In energy calculations 9.5 and 12.5 Å nonbonded cutoff distances (buffer width 0.5 Å) were employed for van der Waals and Coulomb terms, respectively. In a preliminary

MD study (**i**) on the $[H_{-1}\mathbf{L1}]^-$ and $[H_{-1}\mathbf{L2}]^-$ species, performed to evaluate the molecular cavity, the system was allowed to equilibrate for 8 ps, then MD simulations were run for 80 ps with snapshot conformations saved every ps, and a distance-dependent dielectric constant [$\varepsilon(r) = 80r$] was used. The dynamic behavior of the zwitterionic ligand forms, **L1** and **L2**, (**ii**) was investigated by placing the studied species in a cubic cell (25 Å edge) containing SPC model water molecules (equilibration time 8 ps, data collection time 80 ps, snapshot conformations saved every ps). The geometry of the water molecules was fixed by means of the rattle option. Periodic boundary conditions were applied. In addition, calculations on $M[H_{-1}\mathbf{L1}]$ and $M[H_{-1}\mathbf{L2}]$ were performed both by mimicking the solvent with a distance-dependent dielectric constant $\varepsilon(r) = 80r$ [equilibration time 20 ps, data collection time 200 ps, (**iii**)] and by surrounding the solute species with water molecules occupying the volume of a cube (25 Å edge) as previously reported (**iv**).

Spectrophotometric Measurements: Absorption spectra were recorded at 298 K with a Varian Cary-100 spectrophotometer, equipped with a temperature control unit.

Potentiometric Measurements: All potentiometric measurements were carried out in 0.15 mol dm^{-3} Me_4NCl at 298.0±0.1 K, in the pH range 2.4−10.5, using the fully automatic equipment that has already been described.[38] The emf data were acquired with the PASAT computer program.[38] The electrode was calibrated as a hydrogen concentration probe by titrating known amounts of HCl with CO_2-free Me_4NOH solutions and determining the equivalent point by Gran's method,[39] which gives the standard potential E° and the ionic product of water K_w. At least two to three measurements were performed for each ligand. The HYPERQUAD[40] computer programs were used to process the potentiometric data and calculate the protonation constants.

Ligand Synthesis: The precursor reagents **7** and **15** were synthesized as depicted in Figure 6 and Figure 7, respectively. Ligands **L1** and **L2** were obtained according to the synthetic procedure reported in Figure 5. *N*-(*p*-Tolylsulfonyl)aziridine (**2**),[41] bis(2-chloroethyl)methylamine (**5**),[42] 2,6-bis(bromomethyl)anisole (**8**),[43] and **16**[43] were prepared as previously described. The solvents and the starting materials not mentioned were used as purchased. All reactions were carried out under nitrogen.

4,7-Dimethyl-1,10-bis(*p*-tolylsulfonyl)-1,4,7,10-tetraazadecane (3): A solution of *N*-(*p*-tolylsulfonyl)aziridine (6.7 g, 0.034 mol) in anhydrous benzene (200 mL) was added dropwise at room temperature to a stirred solution of *N*,*N*′-dimethyl-1,2-ethylendiamine (3.0 g, 0.034 mol) in anhydrous benzene (400 mL) over a period of 7 h. The resulting solution was kept at room temperature for ca. 12 h and then a further 6.7 g (0.0034 mol) of **2** in 200 mL of benzene was added under the same experimental conditions. After 12 h, the turbid solution was filtered and concentrated under reduced pressure to give the crude compound **3** as a yellowish solid. The product was dissolved in 150 mL of ethanol and an excess of 37% HCl was added to the solution, obtaining **3** as the dihydrochloride salt. Yield: 14.7 g (78%). − $C_{22}H_{36}Cl_2N_4O_4S_2$ (555.6): calcd. C 47.56, H 6.53, N 10.08; found C 47.6, H 6.6, N 10.0. − ^{1}H NMR (D_2O, 25 °C): δ = 2.34 (s, 6 H), 2.94 (s, 6 H), 3.23 (t, 4 H), 3.36 (t, 4 H), 3.67 (s, 4 H), 7.38 (d, 4 H), 7.69 (d, 4 H). − ^{13}C NMR (D_2O, 25 °C): δ = 21.9, 38.7, 42.3, 50.6, 57.1, 128.1, 131.5, 135.1, 146.9.

1,7,10-Trimethyl-4,13-bis(*p*-tolylsulfonyl)-1,4,7,10,13-pentaazacyclopentadecane (6): A solution of sodium (0.96 g, 0.042 mol) in dry ethanol (50 mL) was added to a hot solution of **3**·2HCl (5.6 g, 0.01 mol) in dry ethanol (100 mL). The resulting suspension was refluxed for 30 min, after which time the solvent was removed under reduced pressure. The solid residue was dissolved in dry DMF (50 mL) and to the resulting solution, heated at 110 °C, a solution of bis(2-chloroethyl)methylamine (**5**) (1.6 g, 0.01 mol), dissolved in 100 mL of dry DMF, was added. The reaction mixture was stirred over a period of 4 h. It was kept at 110 °C for a further 2 h. The suspension was then cooled, filtered, and concentrated under reduced pressure to give a yellowish solid, which was chromatographed on neutral alumina using $CHCl_3$ as the eluent. The eluted fractions containing the product having $R_f = 0.77$ were collected and concentrated to dryness, affording **6** as a white solid. Yield: 3.1 g (55%). − $C_{27}H_{43}N_5O_4S_2$ (565.8): calcd. C 57.32, H 7.66, N 12.38; found C 57.5, H 7.7, N 12.5. − MS (FAB): 567 [M + H^+]. − ^{1}H NMR ($CDCl_3$, 25 °C): δ = 2.14 (s, 6 H), 2.37 (s, 3 H), 2.42 (s, 6 H), 2.54 (t, 4 H), 2.67 (t, 4 H), 2.96 (s, 4 H), 3.28 (m, 8 H) 7.28 (d, 4 H), 7.68 (d, 4 H). − ^{13}C NMR ($CDCl_3$, 25 °C): δ = 21.5, 42.5, 43.7, 46.9, 47.4, 55.6, 56.4, 58.4 127.1, 129.7, 136.7, 143.2.

1,7,10-Trimethyl-1,4,7,10,13-pentaazacyclopentadecane (7): A solution of **6** (3.0 g, 0.005 mol) was dissolved in 8 mL of 96% H_2SO_4 and the resulting solution kept at 100 °C for 72 h. The solution was cooled and added to 200 mL of diethyl ether with stirring. It gave a brown solid, which was filtered and washed with diethyl ether. The residue was dissolved in the minimum amount of water and made alkaline with concentrated aqueous NaOH. The Na_2SO_4 precipitate was filtered off and the alkaline solution was extracted with $CHCl_3$ (6 × 100 mL). The organic solutions were combined, dried with Na_2SO_4 and concentrated under reduced pressure to obtain **7** as a colorless oil. Yield: 1.2 g (88%). − $C_{13}H_{31}N_5$ (257.4): calcd. C 60.66, H 12.14, N 27.21; found C 60.5, H 12.3, N 27.0. − ^{1}H NMR ($CDCl_3$, 25 °C): δ = 2.13 (s, 6 H), 2.24 (s, 3 H), 2.41 (m, 8 H), 2.51 (t, 4 H), 2.67 (t, 4 H), 2.76 (s, 4 H),. − ^{13}C NMR ($CDCl_3$, 25 °C): δ = 42.1, 42.4, 47.1, 47.2, 55.6, 57.0, 57.5.

Diethyl 2-{3-[2,2-Bis(ethoxycarbonyl)ethyl]-2-methoxybenzyl}-malonate (10): A solution of **8** (11.8 g, 0.04 mol) in 150 mL of acetonitrile was added to a refluxing suspension of **9** (12.8 g, 0.08 mol) and K_2CO_3 (27.6 g, 0.2 mol) in 300 mL of acetonitrile over a period of 1 h. The reaction mixture was maintained under reflux for a further 3 d. The mixture was then cooled to room temperature and the resulting suspension was filtered and the solution concentrated under reduced pressure, giving the crude product, which was chromatographed on neutral alumina ($CHCl_3$). The eluted fractions ($R_f = 0.79$) were collected and concentrated to dryness, affording **10** as a colorless oil. Yield: 16.7 g (92%). − $C_{23}H_{32}O_9$ (452.5): calcd. C 61.05, H 7.13; found C 60.9, H 7.2. − ^{1}H NMR ($CDCl_3$, 25 °C): δ = 1.20 (t, 12 H), 3.22 (d, 4 H) 3.79 (t, 2 H), 3.81 (s, 3 H), 4.14 (q, 8 H), 6.92(t, 1 H), 7.08 (d, 2 H). − ^{13}C NMR ($CDCl_3$, 25 °C): δ = 13.9, 29.5, 52.1, 60.7, 60.9, 124.1, 129.6, 131.4, 157.7, 169.1.

2-[3-(2,2-Dicarboxyethyl)-2-methoxybenzyl]malonic Acid (11): A solution of **10** (9.0 g, 0.02 mol) and NaOH (12.0 g, 0.3 mol) in 100 mL of ethanol was refluxed for 7 h. The mixture was cooled, 50 mL of ethanol was added. The solution was maintained under stirring for further 12 h. Acetonitrile (80 mL) was added to the resulting deliquescent mixture until the complete precipitation of a white solid was obtained. The dried solid was dissolved in the minimum amount of water and the solution, made acidic with 37% HCl, was extracted with ethyl ether (5 × 30 mL). The organic solutions were combined, dried with Na_2SO_4 and concentrated under reduced pressure to obtain **11** as a colorless oil. Yield: 5.4 g (79%). − $C_{15}H_{16}O_9$ (340.3): calcd. C 52.95, H 4.74; found C 53.1, H 4.8. − ^{1}H NMR ($CDCl_3$, 25 °C): δ = 3.10 (d, 4 H) 3.67 (s, 3 H), 3.77 (t, 2 H), 6.92(t, 1 H), 7.00 (d, 2 H). − ^{13}C NMR ($CDCl_3$, 25 °C): δ = 30.3, 53.5, 62.3, 126.1, 130.8, 132.2, 158.2, 174.2.

3-[3-(2-Carboxyethyl)-2-methoxyphenyl]propionic Acid (12): A solution of **11** (6.8 g, 0.02 mol) and diphenyl ether (150 g) was refluxed for 2 h. The solution was cooled and 50 mL of $CHCl_3$ was added. This solution was then washed with 0.1 mol dm^{-3} NaOH (6 × 25 mL). The collected aqueous part was acidified with 96% H_2SO_4 and the solution extracted with diethyl ether (6 × 25 mL). The organic solutions were combined, dried with Na_2SO_4 and concentrated under reduced pressure to obtain **12** as a yellowish solid. Yield: 3.9 g (77%). − $C_{13}H_{16}O_5$ (252.3): calcd. C 61.90, H 6.39; found C 61.8, H 6.3. − ^{1}H NMR ($CDCl_3$, 25 °C): δ = 2.70 (t, 4 H) 2.99 (t, 4 H), 3.78 (s, 3 H), 7.08 (m, 3 H), 10.32 (b, 2 H). − ^{13}C NMR ($CDCl_3$, 25 °C): δ = 25.2, 34.5, 61.0, 124.5, 128.4, 133.4, 157.1, 179.4.

Ethyl 3-[3-(2-Ethoxycarbonylethyl)-2-methoxyphenyl]propionate (13): A solution of **12** (7.6 g, 0.03 mol) and *p*-toluenesulfonic acid (8.6 g, 0.045 mol) in 100 mL of ethanol was kept under reflux for a period of 12 h. An aqueous solution of $NaHCO_3$ was added to the reaction mixture (cooled to room temperature) until neutralization was achieved. The mixture was extracted with CH_2Cl_2 (3 × 50 mL), and the organic layer was combined, dried with Na_2SO_4 and concentrated under reduced pressure to obtain **13** as an oil. Yield: 8.2 g (89%). − $C_{17}H_{24}O_5$ (308.4): calcd. C 66.21, H 7.84; found C 66.0, H 7.9. − ^{1}H NMR ($CDCl_3$, 25 °C): δ = 1.25 (t, 6 H), 2.62 (t, 4 H), 2.98 (t, 4 H), 3.77 (s, 3 H), 4.14 (q, 4 H), 7.02 (m, 3 H). − ^{13}C NMR ($CDCl_3$, 25 °C): δ = 14.2, 25.5, 34.9, 60.4, 61.3, 124.3, 128.2, 133.8, 157.3, 173.2.

3-[3-(3-Hydroxypropyl)-2-methoxyphenyl]propanol (14): A solution of **13** (6.2 g, 0.02 mol) in 50 mL of anhydrous diethyl ether was carefully added to a suspension of $LiAlH_4$ in 100 mL of anhydrous ethyl ether. The mixture was allowed to react for 3 h at room temperature. An aqueous solution of $NaHCO_3$ was added to the mixture until excess $LiAlH_4$ was completely destroyed. The suspension was extracted with $CHCl_3$ (6 × 50 mL) and the organic solutions were combined, dried with Na_2SO_4 and concentrated under reduced pressure to obtain **14** as a yellowish oil. Yield: 4.1 g (91%). − $C_{13}H_{20}O_3$ (224.3): calcd. C 69.61, H 8.99; found C 69.7, H 9.1. − ^{1}H NMR ($CDCl_3$, 25 °C): δ = 1.87 (q, 4 H), 2.34 (s, 2 H), 2.75 (t, 4 H), 3.58 (t, 4 H), 3.78 (s, 3 H), 7.05 (m, 3 H). − ^{13}C NMR ($CDCl_3$, 25 °C): δ = 25.7, 33.5, 61.4, 61.6, 124.8, 128.3, 134.5, 156.5.

Methyl 3-[2-Methoxy-3-(3-methylsulfonyloxypropyl)phenyl]propylsulfonate (15): A solution of methylsulfonyl chloride in anhydrous CH_2Cl_2 (40 mL) was added to an ice-cold solution of **14** (4.0 g, 0.018 mol) and triethylamine in 50 mL of anhydrous CH_2Cl_2, over a period of 1 h. The solution was kept at this temperature for a further 2 h, and then washed with 5% HCl aqueous solution (3 × 50 mL), 10% $NaHCO_3$ aqueous solution (3 × 50 mL) and water (3 × 50 mL). The organic part was dried with Na_2SO_4 and concentrated under reduced pressure to give **15** as an oil. Yield: 6.5 g (95%). − $C_{15}H_{24}O_7S_2$ (380.5): calcd. C 47.35, H 6.36; found C 47.2, H 6.5. − ^{1}H NMR ($CDCl_3$, 25 °C): δ = 2.09 (q, 4 H), 2.77 (t, 4 H), 3.01 (s, 6 H), 3.74 (s, 3 H), 4.24 (t, 4 H), 7.06 (m, 3 H). − ^{13}C NMR ($CDCl_3$, 25 °C): δ = 26.0, 29.9, 37.3, 61.2, 69.6, 124.5, 128.6, 133.7, 156.7.

Cryptand 18 (18·4HCl): Amine **7** (1.3 g, 5 mmol) and Na_2CO_3 (2.65 g, 25 mmol) were suspended in refluxing CH_3CN (100 mL). To this mixture, a solution of **15** (1.8 g, 5 mmol) in CH_3CN (100 mL) was added dropwise over 6 h, after which the suspension was refluxed for 72 h and then filtered. The solution was concentrated under vacuum to yield the crude product, which was chromatographed on neutral alumina ($CHCl_3$/CH_3OH, 100:4). The eluted fractions were collected and concentrated to yield an oil, which was dissolved in ethanol and treated with 37% hydrochloride acid to give **18** as a tetrahydrochloride salt (1.2 g, 42%). − $C_{24}H_{47}Cl_4N_5O$ (**18**·4HCl: 563.5): calcd. C 51.16, H 8.41, N 12.43; found C 51.1, H 8.3, N 12.3. − MS (FAB), *m*/*z*: 419 [M + H^+]. − ^{13}C NMR: δ = 25.8, 29.7, 43.2, 43.3, 44.6, 52.3, 52.7, 53.8, 55.3, 56.1, 62.0, 64.1, 127.2, 128.3, 129.6, 131.5, 135.3, 157.5, 158.2.

Cryptand L2 (L2·4HCl): A solution of cryptand **18**·4HCl (1.1 g, 2 mmol), EtSNa (1.7 g, 20 mmol) and LiBr (0.51 g, 6 mmol) in dry DMF (50 mL) was heated at 150 °C for 6 h. The solvent was then vacuum-evaporated and the residue was suspended in CH_2Cl_2 and filtered. The organic layer was concentrated and the crude product was chromatographed on neutral alumina (CH_2Cl_2/MeOH, 100:1). The eluted fractions were collected and concentrated to dryness. The crude product was dissolved in ethanol and treated with 37% hydrochloric acid to give the **L2** tetrahydrochloride salt as a white solid (0.69 g, 63%). − $C_{23}H_{45}Cl_4N_5O$ (**L2**·4HCl: 549.5): calcd. C 50.28, H 8.25, N 12.75; found C 55.3, H 8.4, N 12.6. − ^{1}H NMR (D_2O, pH = 7): δ = 2.32 (s, 3 H) 2.63 (s, 6 H), 3.28 (b, 28 H), 6.72 (t, 1 H), 7.02 (d, 2 H). − ^{13}C NMR (D_2O, pH = 7): δ = 30.4, 41.5, 41.7, 52.1, 54.9, 55.3, 56.0, 58.8, 120.7, 129.1, 131.7, 156.5.

Cryptand 19 (19·2HClO$_4$): This compound was synthesized from amine **17** (2.0 g, 0.01 mol), Na_2CO_3 (5.3 g, 0.05 mol) and **15** (3.5 g, 0.01 mol) according to the same procedure reported for **18**. The crude product **17** was dissolved in ethanol and treated with 65% perchloric acid to give the diperchlorate salt as a white solid (2.3 g, 39%). − $C_{23}H_{42}Cl_2N_4O_9$ (**19**·2$HClO_4$: 589.5): calcd. C 48.86, H 7.18, N 9.50; found C 48.9, H 7.1, N 9.4. − MS (FAB), *m*/*z*: 390 [M + H^+]. − ^{1}H NMR (D_2O, pH = 7, 25° C): δ = 2.14 (b, 4 H), 2.36 (s, 6 H), 2.83 (b, 16 H), 3.19 (b, 4 H), 3.39 (b, 4 H), 3.80 (s, 3 H), 7.27 (m, 3 H). − ^{13}C NMR (D_2O, pH = 7, 25° C): δ = 25.2, 29.0, 43.6, 45.2, 49.4, 52.8, 53.4, 54.0, 55.6, 62.2, 127.1, 130.2, 136.1, 157.2.

Cryptand L1 (L1·3HCl): This compound was synthesized from cryptand **19**·2$HClO_4$ (1.2 g, 2 mmol), according to the same procedure reported for **L2**. The crude product **L1** was dissolved in ethanol and treated with 37% hydrochloric acid to give the trihydrochloride salt as a white solid (0.57 g, 59%). − $C_{22}H_{41}Cl_3N_4O$ (**L1**·3HCl: 484.0): calcd. C 54.60, H 8.54, N 11.58; found C 54.5, H 8.7, N 11.4. − ^{1}H NMR (D_2O, pH = 3): δ = 2.03 (m, 4 H) 2.66 (s, 6 H), 2.76 (m, 16 H), 3.16 (m, 8 H), 6.99 (t, 1 H), 7.14 (d, 2 H). − ^{13}C NMR (D_2O, pH = 3): δ = 25.7, 29.4, 44.6, 49.8, 53.7, 54.4, 124.3, 130.2, 132.6, 156.2.

Preparation of the Complexes. − [LiH$_{-1}$L1]: A solution of LiOH (10 mg, 0.44 mmol) in 15 mL of methanol was added to a solution of **L1**·3HCl_3 (48 mg, 0.1 mmol) in methanol (15 mL). The reaction mixture was stirred for 15 min and then concentrated to dryness. The solid was suspended in 20 mL of $CHCl_3$ and the mixture filtered to separate the inorganic excess. The organic solution was dried with Na_2SO_4. On addition of cyclohexane (25 mL) a white precipitate formed. Yield 31 mg (81%). − $C_{22}H_{37}LiN_4O$ (380.5): calcd. C 69.45, H 9.80, N 14.72; found C 69.3, H 9.7, N 14.6. − ^{13}C NMR ($CDCl_3$): δ = 29.9, 34.2, 43.7, 54.3, 55.5, 59.3, 119.5, 129.4, 132.7, 160.4. − **[NaL2]:** An excess of $NaClO_4$ was added to a solution of **L2**·4HCl (165 mg, 0.3 mmol) in 50 mL of water. A 0.1 mol dm^{-3} NaOH solution was added until complete precipitation of a white precipitate was obtained. The solid was then suspended in 20 mL of $CHCl_3$ and the mixture filtered. The liquid part was dried with Na_2SO_4 and concentrated to dryness. The solid was recrystallized by slow concentration of a mixture of $CHCl_3$/cyclohexane, obtaining white crystals suitable for X-ray analysis.

Yield 60 mg (38%). − $C_{23}H_{41}ClN_5NaO_5$ (526.1): calcd. C 52.51, H 7.86, N 13.31; found C 52.6, H 7.9, N 13.2. − ^{13}C NMR ($CDCl_3$): δ = 30.6, 42.7, 42.9, 55.3, 56.7, 58.3, 58.6, 63.0, 121.1, 127.4, 133.0, 153.8. − **[NaH$_{-1}$L2]:** This compound was synthesized from [Na**L2**] (53 mg, 0.1 mmol) according to the same procedure reported for [LiH$_{-1}$**L1**], giving [NaH$_{-1}$**L2**] as a white solid. Yield: 30 mg, 69%). − $C_{23}H_{40}N_5NaO$ (425.6): calcd. C 64.91, H 9.47, N 16.46; found C 64.3, H 9.3, N 16.4. − ^{13}C NMR (CD_3OD): δ = 29.1, 31.3, 41.2, 41.8, 43.1, 43.2, 52.6, 54.4, 54.5, 57.1, 57.2, 57.3, 57.5, 58.2, 59.3, 60.9, 66.7, 111.2, 114.69, 127.2, 128.7, 130.7, 132.4, 163.2, 163.4.

Cambridge Structural Database Search: The Cambridge Structural Database (CCDC) V5.19 was used to retrieve structural information about the penta- and hexacoordinated complexes of lithium, sodium and potassium by nitrogen and/or oxygen atoms. The VISTA V2.1 software was used to analyze the retrieved fragments.

X-ray Crystallographic Studies: Cell parameters and intensity data for the two structures were obtained with a Siemens P4 diffractometer, using graphite-monochromated Cu-K_α radiation (λ = 1.54184 Å). Cell parameters were determined by least-squares fitting of 25 centered reflections. The intensities of three standard reflections were measured every 60 min to check the stability of the diffractometer and the decay of the crystals. Intensity data were corrected for Lorentz and polarization effects, and an absorption correction was applied once the structure had been solved by using the Walker and Stuart method.[44] The two structures were solved using the SIR-97 program[45] and subsequently refined by the full-matrix least-squares program SHELX-97.[46] Protonation hydrogen atoms of ligand **L1** were found in difference syntheses and their positions were refined, as well as their isotropic displacement parameters. The other hydrogen atoms of the molecule were introduced in calculated positions and their coordinates refined in agreement with those of the linked atoms [overall isotropic temperature factor U = 0.048(2) Å^2]. The H10 atom of compound **L2** was found in a difference synthesis and its position was refined, as well as its thermal parameter. The other hydrogen atoms of the complex were introduced in calculated positions and their coordinates refined in agreement with those of the linked atoms [U = 0.0126(3) Å^2]. All the non-hydrogen atoms of the two structures were refined anisotropically. Atomic scattering factors and anomalous dispersion corrections for all the atoms were taken from ref.[47] Geometrical calculations were performed using PARST97.[48] The molecular plot was produced by the ORTEP program.[33] Crystallographic data (excluding structural factors) for the structures reported in this paper have been deposited at the Cambridge Crystallographic Data Centre as supplementary publication no. CCDC-152533 and -152534 for [H**L1**](ClO_4) and [Na**L2**](ClO_4), respectively. Copies may be obtained without charge from CCDC, Union Road, Cambridge CB2 1EZ, UK [Fax: (internat.) + 44-1223/336-033; E-mail: deposit@ccdc.cam.ac.uk].

Acknowledgments

Support for this research from MURST (Ministero per l'Università e la Ricerca Scientifica e Tecnologica, COFIN98) and CNR (Consiglio Nazionale delle Ricerche) is gratefully acknowledged.

[1] R. M. Izatt, J. J. Christensen, *Synthetic Multidentate Macrocyclic Ligands*, Academic Press, New York, **1978**.
[2] L. F. Lindoy, *The Chemistry of Macrocyclic Ligands Complexes*, Cambridge University Press, **1989**.
[3] A. Bianchi, M. Micheloni, P. Paoletti, *Coord. Chem. Rev.* **1991**, *101*, 17.
[4] [4a] J. S. Bradshaw, *Aza-Crown Macrocycles*, Wiley, New York, **1993**. − [4b] R. M. Izatt, K. Pawlak, J. S. Bradshaw, R. L. Bruening, *Chem. Rev.* **1991**, *91*, 1721.
[5] [5a] G. W. Gokel, "Crown Ethers and Cryptands" in *Monographs in Supramolecular Chemistry* (Ed.: J. F. Stoddart), The Royal Society of Chemistry, Cambridge, **1992**. − [5b] A. F. Sholl, I. O. Sutherland, *J. Chem. Soc., Chem. Commun.* **1992**, 1252.
[6] [6a] M. Ciampolini, N. Nardi, B. Valtancoli, M. Micheloni, *Coord. Chem. Rev.* **1992**, *120*, 223. − [6b] A. Bencini, V. Fusi, C. Giorgi, M. Micheloni, N. Nardi, B. Valtancoli, *J. Chem. Soc., Perkin Trans. 2* **1996**, 2297. − [6c] M. Formica, V. Fusi, M. Micheloni, R. Pontellini, P. Romani, *Coord. Chem. Rev.* **1999**, *184*, 347 and refs. therein.
[7] H. J. Schneider, A. Yatsimirsky, *Principles and Methods in Supramolecular Chemistry*, Wiley, Chichester, **2000**.
[8] S. Chimichi, M. Ciampolini, P. Dapporto, M. Micheloni F. Vizza, F. Zanobini, *J. Chem. Soc., Dalton Trans.* **1986**, 505.
[9] M. Ciampolini, S. Mangani, M. Micheloni, P. Orioli, F. Vizza, F. Zanobini, *Gazz. Chim. Ital.* **1986**, *116*, 189.
[10] A. Bianchi, E. Garcia-España, M. Micheloni, N. Nardi, F. Vizza, *Inorg. Chem.* **1986**, *25*, 4379.
[11] A. Bianchi, S. Chimichi, M. Ciampolini, M. Micheloni, F. Vizza, *Gazz. Chim. Ital.* **1987**, *117*, 499.
[12] A. Bianchi, M. Ciampolini, E. Garcia-España, S. Mangani, M. Micheloni, N. Nardi, J. A. Ramirez, B. Valtancoli, *J. Chem. Soc., Perkin Trans. 2* **1989**, 1131.
[13] A. Bencini, A. Bianchi, A. Borselli, M. Ciampolini, P. Dapporto, E. Garcia-España, M. Micheloni, N. Nardi, P. Paoli, J. A. Ramirez, B. Valtancoli, *Inorg. Chem.* **1989**, *28*, 4279.
[14] A. Bencini, A. Bianchi, A. Borselli, M. Ciampolini, P. Dapporto, E. Garcia-España, M. Micheloni, P. Paoli, J. A. Ramirez, B. Valtancoli, *J. Chem. Soc., Perkin Trans. 2* **1990**, 209.
[15] [15a] A. Bencini, A. Bianchi, A. Borselli, S. Chimichi, M. Ciampolini, P. Dapporto, M. Micheloni, N. Nardi, P. Paoli, B. Valtancoli, *J. Chem. Soc., Chem. Commun.* **1990**, 174 − [15b] A. Bencini, A. Bianchi, A. Borselli, S. Chimichi, M. Ciampolini, P. Dapporto, M. Micheloni, N. Nardi, P. Paoli, B. Valtancoli, *Inorg. Chem.* **1990**, *29*, 3282.
[16] M. Micheloni, N. Nardi, B. Valtancoli, *Gazz. Chim. Ital.* **1991**, *121*, 29.
[17] A. Bencini, A. Bianchi, S. Chimichi, M. Ciampolini, P. Dapporto, E. Garcia-España, M. Micheloni, N. Nardi, P. Paoli, B. Valtancoli, *Inorg. Chem.* **1991**, *30*, 3687.
[18] A. Bencini, A. Bianchi, M. Ciampolini, P. Dapporto, M. Micheloni, N. Nardi, P. Paoli, B. Valtancoli, *J. Chem. Soc., Perkin Trans. 2* **1992**, 181.
[19] C. Bazzicalupi, A. Bencini, A. Bianchi, M. Ciampolini, P. Dapporto, V. Fusi, M. Micheloni, N. Nardi, P. Paoli, B. Valtancoli, *J. Chem. Soc., Perkin Trans. 2* **1993**, 115.
[20] A. Bencini, A. Bianchi, P. Dapporto, V. Fusi, E. Garcia-España, M. Micheloni, P. Paoletti, P. Paoli, A. Rodriguez, B. Valtancoli, *Inorg. Chem.* **1993**, *32*, 2753.
[21] C. Bazzicalupi, A. Bencini, A. Bianchi, M. Ciampolini, V. Fusi, M. Micheloni, N. Nardi, P. Paoli, B. Valtancoli, *Supramolecular Chem.* **1994**, *3*, 141.
[22] A. Bencini, V. Fusi, C. Giorgi, M. Micheloni, N. Nardi, B. Valtancoli, *J. Chem. Soc., Perkin Trans. 2* **1996**, 2297.
[23] C. Bazzicalupi, A. Bencini, M. Ciampolini, V. Fusi, M. Micheloni, N. Nardi, I. Razzolini, B. Valtancoli, *Supramolecular Chem.* **1996**, 61.
[24] P. Dapporto, V. Fusi, M. Micheloni, P. Palma, P. Paoli, R. Pontellini, *Inorg. Chim. Acta* **1998**, *275*, 168.
[25] E. Bardazzi, M. Ciampolini, V. Fusi, M. Micheloni, N. Nardi, R. Pontellini, P. Romani, *J. Org. Chem.* **1999**, *64*, 1335.
[26] P. Dapporto, V. Fusi, C. Giorgi, M. Micheloni, P. Palma, P. Paoli, R. Pontellini, *Supramolecular Chem.* **1999**, *10*, 243.
[27] M. Micheloni, M. Formica, V. Fusi, P. Romani, R. Pontellini,

P. Dapporto, P. Paoli, P. Rossi, B. Valtancoli, *Eur. J. Inorg. Chem.* **2000**, 51.
[28] F. H. Allen, O. Kennard, Cambridge Structural Database, *Chem. Des. Autom. News* **1993**, *8*, 31.
[29] C. Bazzicalupi, P. Dapporto, V. Fusi, P. Paoli, N. Nardi, B. Valtancoli, *Supramolecular Chem.* **1996**, *7*, 195.
[30] A. Abou-Hamdan, A. M. Hounslow, S. F. Lincoln, T. W. Hambley, *J. Chem. Soc., Dalton Trans.* **1987**, 489.
[31] C. Meiners, M. Nieger, F. Voegtle, *Liebigs Ann.* **1996**, *2*, 297.
[32] L. D. Pettit, *IUPAC − Stability Constants Database*, Academic Software, Yorks, **1994**.
[33] C. K. Johnson, *ORTEP*, Rep. ORNL 3794, Oak Ridge National Laboratory, TN, USA, **1971**.
[34] I. Bernal (Ed.), *Stereochemical and Stereophysical Behaviour of Macrocycles*, Elsevier, Amsterdam, **1987**, p.34.
[35] Biosym/MSI, 9685 Scranton Road, San Diego, CA 92121-3752, USA.
[36] S. J. Weiner, P. A. Kollman, D. A. Case, U. C. Singh, C. Ghio, G. Alagona, S. Profeta, Jr., P. Weiner, *J. Am. Chem. Soc.* **1984**, *106*, 765.
[37] M. J. Frisch, G. W. Trucks, H. B. Schlegel, P. M. W. Gill, B. G. Johnson, M. A. Robb, J. R. Cheeseman, T. A. Keith, G. A. Petersson, J. A. Montgomery, K. Raghavachari, M. A. Al-Laham, V. G. Zakrzewski, J. V. Ortiz, J. B. Foresman, J. Cioslowski, B. B. Stefanov, A. Nanayakkara, M. Challacombe, C. Y. Peng, P. Y. Ayala, W. Chen, M. W. Wong, J. L. Andres, E. S. Replogle, R. Gomperts, R. L. Martin, D. J. Fox, J. S. Binkley, D. J. Defrees, J. Baker, J. P. Stewart, M. Head-Gordon, C. Gonzalez, J. A. Pople, Gaussian, Inc., Pittsburgh PA, **1995**.
[38] M. Fontanelli, M. Micheloni, *1st Spanish-Italian Conf. Thermodynamics of Metal Complexes*, Peñiscola, Univ. of Valencia, Spain, p. 41, June 3−6 **1990**.
[39] [39a] G. Gran, *Analyst* **1952**, *77*, 661 − [39b] F. J. Rossotti, H. Rossotti, *J. Chem. Edu.* **1996**, *43*, 1739.
[40] P. Gans, A. Sabatini, A. Vacca, *Talenta* **1996**, *43*, 1739.
[41] A. E. Martin, T. M. Ford, J. E. Bulkowski, *J. Org. Chem.* **1982**, *47*, 412.
[42] K. Ward, *J. Am. Chem. Soc.* **1935**, *57*, 914.
[43] W. Zazulak, E. Chapoteau, B. P. Czech, A. Kumar, *J. Org. Chem.* **1992**, *25*, 6720.
[44] N. Walker, D. D. Stuart, *Acta Crystallogr., Sect. A* **1983**, *39*, 158.
[45] A. Altomare, G. Cascarano, C. Giacovazzo, A. Guagliardi, M. C. Burla, M. C.; G. Polidori, M. Camalli, *J. Appl. Crystallogr.* **1994**, *27*, 435.
[46] G. M. Sheldrick, *SHELXL-97*, University of Göttingen, Germany, **1997**.
[47] *International Tables for X-ray Crystallography*, Kynoch Press, Birmingham, UK, **1974**, vol.4.
[48] M. Nardelli, *Comput. Chem.* **1983**, *7*, 95.

Received November 22, 2000
[I00443]